PCCP

PAPER

View Article Online
View Journal | View Issue

Cite this: *Phys. Chem. Chem. Phys.*, 2017, **19**, 2479

Pentagonal five-center four-electron π bond in ternary $B_3N_2H_5$ cluster: an extension of the concept of three-center four-electron ω bond†

Da-Zhi Li,‡*[a] Lin-Yan Feng,‡[b] Ling Pei,[a] Li-Juan Zhang,[a] Shu-Guo Wu[a] and Hua-Jin Zhai*[bc]

Received 21st November 2016,
Accepted 16th December 2016

DOI: 10.1039/c6cp07954g

www.rsc.org/pccp

Boron-based heteroatomic rings can have exotic chemical bonding, in which the p lone-pairs of heteroatoms manage to participate in delocalized π bonding, compensating for boron's electron-deficiency. We explore herein the bonding properties of ternary B–N–H systems with a pentagonal ring, using the $B_3N_2H_5^{0/-/2-}$ clusters as examples. Computational structural searches lead to perfectly planar C_{2v} $B_3N_2H_5$ (**1**, $^1A_1$) and C_{2v} $B_3N_2H_5^-$ (**2**, $^2B_1$) as global minima for the neutral species and monoanion, which feature a pentagonal B_3N_2 ring. The corresponding dianion C_{2v} $B_3N_2H_5^{2-}$ (**3**, $^1A_1$) is a local minimum, whose global minimum adopts a chain-like open structure. Bonding analyses reveal a five-center four-electron (5c–4e) π system in **1**, dubbed the 5c–4e o-bond. It is a 4π system in the bonding/nonbonding combination, originating from two N 2p lone-pairs, which can be considered as an extension of the concept of 3c–4e ω-bond. The extra electrons in **2** and **3** occupy a markedly destabilized π orbital. Thus, a 4π configuration, rather than a π sextet according to the $(4n + 2)$ Hückel rule, is electronically robust for the $B_3N_2H_5^{0/-/2-}$ system. Infrared and photoelectron spectra are predicted for **1** and **2**, respectively. Structural evolution of ring-like and chain-like isomers with charge-state in $B_3N_2H_5^{0/-/2-}$ is elucidated. $B_3N_2H_5^-$ (**2**) is used as ligand for sandwich-type complexes: C_{2h} $[(B_3N_2H_5)_2Fe]^{2-}$ and C_{2h} $[(B_3N_2H_5)_2Fe]Li_2$.

1. Introduction

Boron as a neighbor of carbon in the periodic table is electron-deficient, resulting in unusual structural, electronic, and bonding properties for boron-based nanoclusters and nanomaterials. Theoretical and experimental studies have established an analogous relationship between boron-based clusters and aromatic hydrocarbons, including polycyclic aromatic hydrocarbons. Notably, classical inorganic benzene analogues, boroxine ($B_3O_3H_3$) and borazene ($B_3N_3H_6$), have received consistent attention.[1–8] Both $B_3O_3H_3$ and $B_3N_3H_6$ possess a hexagonal B_3X_3 (X = O or N) ring as the structural core, featuring a π sextet akin to benzene. Recently, a D_{3h} B_6O_6 cluster,[9] named "boronyl boroxine" and readily formulated as $B_3O_3(BO)_3$, was shown to be an inorganic benzene or boroxine. Boronyl boroxine can be obtained from boroxine upon substituting the H terminals with three boronyl (BO) groups.[10] Indeed, BO and H are isoelectronic, monovalent σ radicals. Similar to benzene, D_{3h} $B_3O_3X_3$ (X = BO, H) were explored as ligands to form sandwich-type complexes D_{3d} $(B_3O_3X_3)_2Cr$,[9] D_{3d} $(B_3O_3X_3)_2V$,[11a] and perfectly planar $(B_3O_3H_3)_nM^+$ (n = 1, 2; M = Cu, Ag, Au).[11b]

Shrinking the size of the B_3X_3 ring, one can reach rhombic B_2X_2 (X = O, S, N), which were confirmed as the structural core in boron-containing compound clusters, dating back as early as the 1970s: C_{2v} $B_2N_2H_4$,[12,13] C_{2v} $B_2S_2H_2$ and D_{2h} $B_2O_2H_2$,[14] C_{2v} $B_5O_5^-$,[15] and C_{2v} B_4S_4.[16] Bonding analyses revealed a four-center four-electron (4c–4e) π bond, that is, the o-bond. These clusters are 4π systems in a bonding/nonbonding combination, in contrast to the bonding/antibonding combination in 4π antiaromatic cyclobutadiene (C_4H_4).

Cyclopentadienyl (C_5H_5) is a well-known ligand in compounds such as ferrocene, D_{5h} $(C_5H_5)_2Fe$.[17] It is thus desirable to explore heteroatomic, five-membered B–X ring systems in boron-based clusters. However, such systems have remained scarce. Our recent work uncovered a D_{2h} $B_6S_6^{2-}$ cluster as an analog of naphthalene,

[a] *Binzhou Key Laboratory of Materials Chemistry, Department of Chemical Engineering, Binzhou University, Binzhou 256603, P. R. China. E-mail: ldz005@126.com*
[b] *Nanocluster Laboratory, Institute of Molecular Science, Shanxi University, Taiyuan 030006, P. R. China. E-mail: hj.zhai@sxu.edu.cn*
[c] *State Key Laboratory of Quantum Optics and Quantum Optics Devices, Shanxi University, Taiyuan 030006, P. R. China*

† Electronic supplementary information (ESI) available: Alternative optimized low-lying structures of $B_3N_2H_5^{0/-/2-}$ clusters at B3LYP/aug-cc-pVTZ level, along with their relative energies at B3LYP and single-point CCSD(T) (Fig. S1–S3); structure and bonding of chain-like open isomer of $B_3N_2H_5^{2-}$ (Fig. S4 and S5); and optimized sandwich structures C_{2h} $[(B_3N_2H_5)_2Ni]$ (^1A_g) and C_{2v} $[(B_3N_2H_5)_2Ni]$ ($^1A_1$) at B3LYP level (Fig. S6). See DOI: 10.1039/c6cp07954g

‡ D. Z. Li and L. Y. Feng contributed equally to this work.

featuring twin B_3S_2 rings.[18a] Inspired by this finding, we further studied smaller $B_3S_2H_3^{0/-/2-}$ clusters, which were shown to be analogs of cyclopentadienyl and cyclopentadienyl anion (D_{5h} $C_5H_5^-$).[18b]

So, how far can we push the bonding analogy between heteroatomic B–X rings and cyclopentadienyl radical/cyclopentadienyl anion? Does the difference in electronegativity between B and X have a marked effect on the bonding nature of B–X rings? Does the Hückel rule govern the stability of B–X rings in extreme cases? Is the π sextet essential for pentagonal B–X rings? The current work attempts to address these issues. We have studied a series of boron–nitrogen hydride clusters, $B_3N_2H_5^{0/-/2-}$, at three charge-states. The species are isovalent to $C_5H_5^+/C_5H_5/C_5H_5^-$ and $B_3S_2H_3^{0/-/2-}$, but differ from the latter systems in terms of electronegativity: 2.55 for C, 2.04/2.58 for B/S, and 2.04/3.04 for B/N. For the ternary B–N–H clusters, the neutral species and monoanion possess global-minimum structures with a pentagonal B_3N_2 ring: C_{2v} $B_3N_2H_5$ (**1**, $^1A_1$) and C_{2v} $B_3N_2H_5^-$ (**2**, $^2B_1$). The dianion has a pentagonal local minimum C_{2v} $B_3N_2H_5^{2-}$ (**3**, $^1A_1$), whose global minimum is chain-like. $B_3N_2H_5$ (**1**) has an energy gap of 5.42 eV between its highest occupied and lowest unoccupied molecular orbitals (HOMO and LUMO), which indicates a remarkably stable neutral cluster with a 4π system, in contrast to 6π aromaticity according to the $(4n + 2)$ Hückel rule. The robust 4π system in **1** is proposed as a 5c–4e σ-bond. It makes use of two N 2p lone-pairs for a completely bonding five-center π bond and a residual nonbonding one. The 5c–4e σ-bond can be viewed as an extension of the 3c–4e ω-bond in XeF_2.[19]

2. Computational methods

Global-minimum searches for the $B_3N_2H_5$ cluster were conducted at the density-functional theory (DFT) level using the Coalescence Kick (CK)[20,21] and Gradient Embedded Genetic Algorithm (GEGA)[22,23] programs, further aided with manual structural constructions. Structures for $B_3N_2H_5^-$ anion and $B_3N_2H_5^{2-}$ dianion were computed primarily on the basis of low-lying isomers of $B_3N_2H_5$. Considering the connections of the potential energy surfaces in $B_3N_2H_5^{0/-/2-}$, additional computer searches for $B_3N_2H_5^-$ and $B_3N_2H_5^{2-}$ do not seem necessary. Candidate low-lying structures were then fully optimized at the B3LYP/aug-cc-pVTZ level.[24,25] Harmonic vibrational frequencies were calculated at the same level to verify that the reported structures are true minima. Relative energies for top low-lying isomers of $B_3N_2H_5^{0/-/2-}$ were refined using single-point CCSD(T) calculations[26–28] at the B3LYP geometries. For the sandwich complexes, the Stuttgart relativistic small core basis set and effective core potential (Stuttgart RSC 1997 ECP)[29] were employed for Fe and Ni. Structural optimizations were performed for the complexes by taking into consideration different spin-multiplicity states.

Adaptive natural density partitioning (AdNDP)[30] and canonical molecular orbital (CMO) analyses, as well as nucleus-independent chemical shift (NICS)[31] calculations, were carried out to elucidate the nature of bonding and aromaticity in $B_3N_2H_5^{0/-/2-}$. The NBO 5.0 program[32] was used to calculate natural atomic charges. The photoelectron spectrum of the $B_3N_2H_5^-$ (**2**) monoanion cluster was simulated at the time-dependent B3LYP (TD-B3LYP)[33,34] level and the infrared (IR) spectrum predicted for the $B_3N_2H_5$ (**1**) neutral species. All the calculations and analyses were performed using Gaussian 09.[35] Multiwfn[36] was used to perform the orbital composition analysis.

3. Results

Fig. 1 shows the C_{2v} global-minimum structures of $B_3N_2H_5$ (**1**, $^1A_1$) and $B_3N_2H_5^-$ (**2**, $^2B_1$), where **1** is identified from the CK and GEGA searches and **2** is obtained using low-lying isomers of $B_3N_2H_5$ as initial structures by adding one extra electron, followed by structural reoptimizations and energetics evaluation (including CCSD(T)). Also shown is a relevant C_{2v} local minimum for the dianion: $B_3N_2H_5^{2-}$ (**3**, $^1A_1$). Alternative low-lying isomers of $B_3N_2H_5^{0/-/2-}$ within 30 kcal mol^{-1} are presented in the ESI† (Fig. S1–S3).

3.1. $B_3N_2H_5$

As shown in Fig. 1 and Fig. S1 (ESI†), C_{2v} $B_3N_2H_5$ (**1**, $^1A_1$) is global minimum for the neutral species. Structure **1** is perfectly planar and has a pentagonal heteroatomic B_3N_2 ring, terminated by H atoms akin to cyclopentadienyl. The closest competitive structure, C_{2v} ($^1A_1$), has a rhombic B_2N_2 core, which is terminated by three H atoms and one BH_2 group. It is marginally higher in energy by 0.56 kcal mol^{-1} at B3LYP. In fact, the B_2N_2 ring is common in low-lying isomers of $B_3N_2H_5^{0/-}$ (Fig. S1 and S2, ESI†). However, at single-point CCSD(T) level, **1** is better defined as

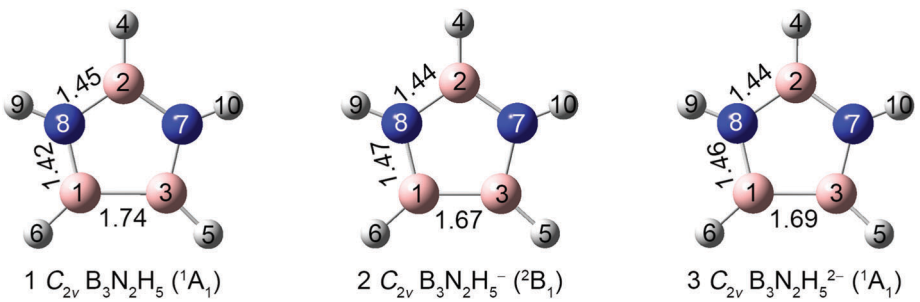

Fig. 1 Global-minimum structures of C_{2v} $B_3N_2H_5$ (**1**, $^1A_1$) and C_{2v} $B_3N_2H_5^-$ (**2**, $^2B_1$) at the B3LYP/aug-cc-pVTZ level, along with a local minimum of C_{2v} $B_3N_2H_5^{2-}$ (**3**, $^1A_1$). These structures possess a heteroatomic B_3N_2 five-membered ring. Selected bond distances are labeled in Angstroms. The B atom is in pink, N in blue, and H in gray.

global minimum, with alternative structures being at least 4.8 kcal mol^{-1} higher in energy.

Recommended covalent radii[37] give the upper bound of B–B single, B=B double, and B≡B triple bonds as 1.70, 1.56, and 1.46 Å, respectively. The B1–B3 distance in **1** (1.74 Å) is close to and somewhat longer than a single bond; we tentatively assign it as a single bond. The B–N distances are 1.42 and 1.45 Å, which are in between single (1.56 Å) and double (1.38 Å) bonds, suggesting a delocalized ring system. The calculated HOMO–LUMO gap of **1** is 5.42 eV at B3LYP, confirming a robust, closed-shell electronic system.

3.2. $B_3N_2H_5^-$

Adding one extra electron to the LUMO of **1**, we reach the C_{2v} $B_3N_2H_5^-$ (**2**, $^2B_1$) monoanion. It turns out to be the global minimum (Fig. S2, ESI†), which lies 9.66 and 18.09 kcal mol^{-1} below the second isomer, C_s ($^2A''$), at B3LYP and single-point CCSD(T) levels, respectively. Note that the rhombic isomer for the monoanion, C_{2v} ($^2B_1$), is 17.36 kcal mol^{-1} above the global minimum at B3LYP, in sharp contrast to the neutral system (0.56 kcal mol^{-1}; Fig. S1, ESI†).

The B1–B3 distance in **2** is 1.67 Å, being shorter by 0.07 Å than that in **1**, suggesting that the former is probably beyond a single bond. The B–N bonds in **2** are 1.44 *versus* 1.47 Å, which both fall in between single and double bonds, similar to **1**. However, the bottom B–N bonds (B1–N8 and B3–N7) expand by 0.05 Å from **1** to **2**, whereas the upper ones shrink by 0.01 Å. The distance changes indicate that the extra electron in **2** is heavily located on B1–B3, and that there appears to be substantial intramolecular Coulomb repulsion even in the monoanion.

3.3. $B_3N_2H_5^{2-}$

A cyclic dianion cluster C_{2v} $B_3N_2H_5^{2-}$ (**3**, $^1A_1$) (Fig. 1) is located by adding one electron to the singly-occupied HOMO of **2**. Structure **3** is a true minimum, which lies 20.65 and 12.19 kcal mol^{-1} above a chain-like open structure C_s ($^1A'$) (Fig. S3, ESI†) at B3LYP and CCSD(T), respectively. Structure-wise, **3** is rather similar to **2**, and the B1–B3 distance expands slightly from **2** to **3** despite one more bonding electron in the latter. The potential energy surface of the $B_3N_2H_5^{2-}$ dianion appears to be more complicated than those of the neutral species and monoanion, in particular at the CCSD(T) level, where three chain-like dianion structures are within 1.18 kcal mol^{-1}. Given the computational uncertainties in energetics for the dianion, these structures cannot be distinguished from each other. We thus choose to discuss only the first structure in the text.

4. Discussion

4.1. Structures and bonding in $B_3N_2H_5^{0/-/2-}$: the importance of 4π electrons

The C_{2v} $B_3N_2H_5^{0/-/2-}$ (**1–3**) species have a five-membered B_3N_2 ring as the structural core, similar to the C_5 ring in C_5H_5 and $C_5H_5^-$. In terms of valence electrons, $B_3N_2H_5$ has one fewer than C_5H_5. Thus, **1–3** are formally isovalent to $C_5H_5^{+/0/-}$. Bonding analyses for **1–3** are relatively simple. For example, the bonding

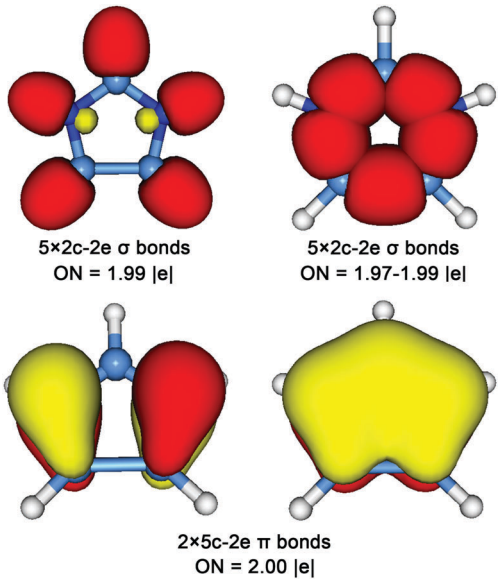

Fig. 2 Bonding pattern of C_{2v} $B_3N_2H_5$ (**1**) neutral cluster on the basis of adaptive natural density partitioning (AdNDP) analysis. Occupation numbers (ONs) are shown.

elements in **1** as revealed from AdNDP are illustrated in Fig. 2. It has 24 electrons, of which 10 are used for five terminal 2c–2e σ B–H bonds and another 10 for four 2c–2e σ B–N bonds and one 2c–2e σ B–B bond. In short, the σ framework consumes 20 electrons for classical, localized bonds. The remaining 4 electrons form the π framework with a completely bonding 5c–2e π bond, as well as a formally bonding/antibonding 5c–2e π bond (Fig. 2, bottom panels), which look similar in shape to two of the π CMOs in a typical π sextet, such as in benzene. All AdNDP bonds in **1** have nearly ideal occupation numbers (ONs): 1.97–2.00 |e|.

Now the question is: is a π sextet (or the Hückel rule) required in order to electronically stabilize the **1–3** system? Fig. 3 compares the orbital energy patterns of C_{2v} $B_3N_2H_5$ (**1**), C_{2v} $B_3S_2H_3$, and D_{5h} $C_5H_5^-$, where C_{2v} $B_3S_2H_3$ with 4π electrons was recently studied as an analog of $C_5H_5^+$ (ref. 18*b*) and $C_5H_5^-$ is known to possess a π sextet. C_{2v} $B_3N_2H_5$ (**1**) differs from C_{2v} $B_3S_2H_3$ and D_{5h} $C_5H_5^-$ in two aspects. First, **1** has a huge energy gap (5.61 eV) between the two π* CMOs: HOMO−1 and LUMO. Thus, the LUMO is substantially destabilized with respect to HOMO, making its monoanion and dianion (**2** and **3**) unfavorable. The primary reason is that HOMO−1 is N based (and hence low in energy), whereas LUMO is B based. Despite the B/N mixture and delocalization, the two π* CMOs cannot be made close in energy or degenerate in **1–3**. For comparison, C_{2v} $B_3S_2H_3$ has a smaller gap of 3.52 eV and D_{5h} $C_5H_5^-$ has a zero gap because two π* CMOs therein are degenerate. Second, in light of the fact that 4π rather than 6π is favorable in **1–3**, the Hückel rule no longer seems to govern the stability of $B_3N_2H_5^{0/-/2-}$.

4.2. On the five-center four-electron (5c–4e) σ-bond in C_{2v} $B_3N_2H_5$: a conceptual extension of the 3c–4e ω-bond

Electron-deficient compounds are known to form 3c–4e ω-bond.[19] For example, XeF_2 as a linear species is held together by a

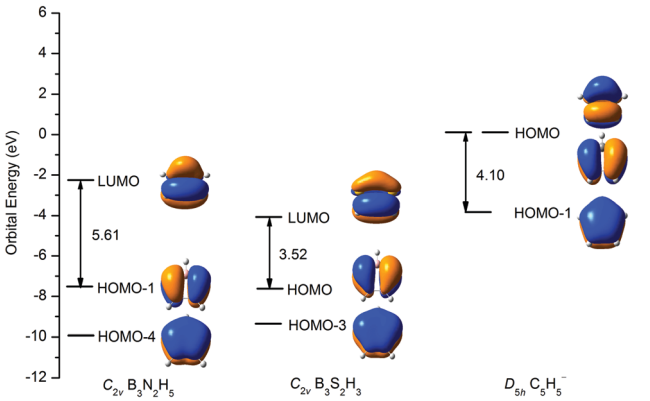

Fig. 3 Comparison of orbital energy levels of π canonical molecular orbitals (CMOs) at the B3LYP/aug-cc-pVTZ level for C_{2v} $B_3N_2H_5$ (**1**) (left panel), C_{2v} $B_3S_2H_3$ (middle), and D_{5h} $C_5H_5^-$ (right).

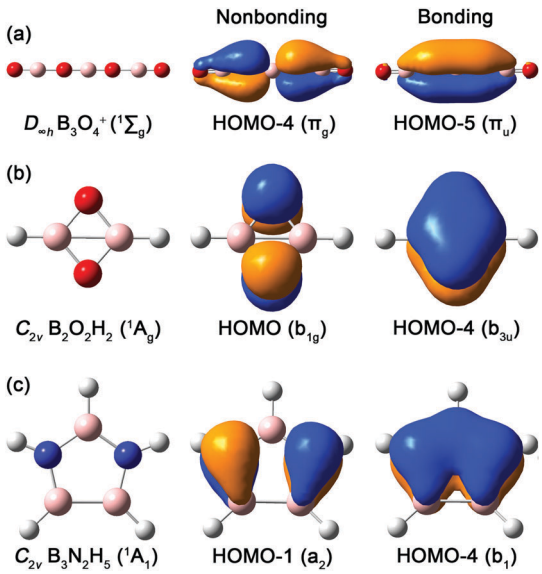

Fig. 4 Canonical molecular orbitals (CMOs) for (c) the five-center four-electron (5c–4e) o-bond in C_{2v} $B_3N_2H_5$ (**1**), as compared with those for (a) the 3c–4e ω-bond in $B_3O_4^+$ (ref. 19) and (b) the 4c–4e o-bond in C_{2v} $B_2O_2H_2$ (ref. 14).

completely bonding CMO and a nonbonding one. Such a bonding/nonbonding combination of σ CMOs is called the 3c–4e ω-bond, leading to an effective Xe–F bond order of 0.5. For boron-based clusters, the 3c–4e ω-bond was recently extended to linear π systems (Fig. 4(a)).[38] Furthermore, the 4π system in clusters with a rhombic B_2O_2 core was described as the 4c–4e o-bond (Fig. 4(b)).[14] The favorable 4π electron-counting in C_{2v} $B_3N_2H_5^{0/-/2-}$ (**1–3**) offers the possibility to further extend the concept of the 3c–4e ω-bond, this time from the linear three-center case to the pentagonal, heteroatomic B_3N_2 ring.

The key to validate this extension lies in the nature of two π CMOs in **1** (Fig. 4(c); Table 1). Here HOMO−4 is a completely bonding π CMO, being contributed by p atomic orbitals (AOs) of N7/N8 (72.8% in total) and yet with substantial contributions from p AOs of B1/B2/B3 (26.9% in total). On the other hand,

Table 1 Orbital composition analysis for the π canonical molecular orbitals (CMOs) of D_{2h} $B_2O_2H_2$ (^1A_g)[a] and C_{2v} $B_3N_2H_5$ (**1**, $^1A_1$)

Species	CMO	O/N (%)	B (%)	O/N (total, %)
C_{2v} $B_2O_2H_2$[b]	HOMO	O5-p 49.7 O6-p 49.7		99.4
	HOMO−4	O5-p 36.7 O6-p 36.7	B1-p 12.9 B2-p 12.9	73.4
C_{2v} $B_3N_2H_5$ (**1**)[c]	HOMO−1	N7-p 45.5 N8-p 45.5	B1-p 4.4 B3-p 4.4	91.1
	HOMO−4	N7-p 36.4 N8-p 36.4	B1-p 6.4 B3-p 6.4 B2-p 14.1	72.8

[a] Structure as optimized in ref. 14. [b] Energy difference between the nonbonding and completely bonding π CMOs is 3.13 eV. [c] The corresponding energy difference is 2.14 eV for this species.

HOMO−1 is dominated by 91.1% contributions from p AOs of N7/N8. Since the N–N distance (2.38 Å; compared with 1.42 Å for N–N single bond[37]) is quite large, the N–N interaction is negligible and HOMO−1 can be practically viewed as nonbonding. In short, HOMO−4 and HOMO−1 in **1** represent a bonding/nonbonding combination of π CMOs, exactly in the spirit of the linear 3c–4e ω-bond[19] and rhombic 4c–4e o-bond.[14] Therefore, we propose to call the 4π system in $B_3N_2H_5$ (**1**) the 5c–4e o-bond.

The 5c–4e o-bond in **1** originates from two N 2p lone-pairs. It makes use of two of these electrons for a completely bonding π CMO owing to the covalent/ionic interaction of B/N centers; two "residual" electrons occupy a nonbonding CMO. The net bonding effect of the 4π electrons is dominated by HOMO−4, thus effectively making it a 2π system (aromatic at least formally).[39] The orbital energy difference between HOMO−4 and HOMO−1 (2.14 eV at B3LYP; Table 1) allows an estimation of the bond strength as ~4.3 eV for the 4π electrons, which is significant in particular considering the fact that they would otherwise be merely two lone-pairs. The concept of the 5c–4e o-bond may be applicable to the C_{2v} $B_3S_2H_3^{0/-/2-}$ system[18b] as well, although this was not recognized in the prior paper. Both C_{2v} $B_3N_2H_5$ and C_{2v} $B_3S_2H_3$ have 4π electrons and may be considered analogs of $C_5H_5^+$.[40]

Heteroatomic systems such as $B_3N_2H_5^{0/-/2-}$ (**1–3**) are known to be less delocalized and hence less aromatic[18b] than prototypical hydrocarbons. However, NICS calculations help elucidate the trend of relevant systems, as summarized in Table 2. Here NICS(1) and $NICS_{zz}(1)$ as a measure of aromaticity are calculated at 1 Å above the ring center. The values for C_{2v} $B_3N_2H_5$ (**1**) at B3LYP are 0.64 and 5.80 ppm, respectively, which are small and insufficient for claim of either aromaticity or antiaromaticity. Nevertheless, the NICS data suggest a rough order of decreasing aromaticity in pentagonal rings as follows: D_{5h} $C_5H_5^-$ > C_{2v} $B_3S_2H_3^{2-}$ > C_{2v} $B_3N_2H_5^{2-}$ (**3**). Not surprisingly, for five-membered ring systems with a π sextet, the larger the electronegativity difference between the heteroatoms, the weaker the aromaticity for the system. Indeed, we also did calculations for the C_{2v} $B_3NSH_4^{2-}$ species, which is isovalent to C_{2v} $B_3S_2H_3^{2-}$ and C_{2v} $B_3N_2H_5^{2-}$ (**3**) but with substitution of one NH group by S.

Table 2 Nucleus-independent chemical shift, NICS(1) and $NICS_{zz}(1)$, for $B_3N_2H_5^{2-}$ and $B_3N_2H_5$, as well as their relevant B–S–H, B–N–S–H, and C–H species, at the B3LYP/aug-cc-pVTZ level. These values are calculated at 1 Å above the ring center

Species[a]	NICS(1) (ppm)	$NICS_{zz}(1)$ (ppm)
C_{2v} $B_3N_2H_5^{2-}$ ($^1A_1$)	**−0.16**	**−1.66**
C_{2v} $B_3N_2H_5$ ($^1A_1$)	0.64	5.80
C_{2v} $B_3S_2H_3^{2-}$ ($^1A_1$)	**−5.06**	**−13.64**
C_{2v} $B_3S_2H_3$ ($^1A_1$)	0.24	6.71
C_{2v} $B_3NSH_4^{2-}$ ($^1A_1$)	**−4.73**	**−11.15**
D_{5h} $C_5H_5^-$ ($^1A_1'$)	**−9.66**	**−34.54**
C_{2v} $C_5H_5^+$ ($^1A_1$)	65.01	198.97

[a] The 6π systems are shown in boldface.

C_{2v} $B_3NSH_4^{2-}$ as a true minimum has calculated NICS(1) and $NICS_{zz}(1)$ values of −4.73 and −11.15 ppm, respectively, which are in between those of C_{2v} $B_3S_2H_3^{2-}$ and C_{2v} $B_3N_2H_5^{2-}$ (**3**). The least aromaticity of C_{2v} $B_3N_2H_5^{2-}$ (**3**) in all species discussed above makes the $B_3N_2H_5^{0/-/2-}$ system an ideal candidate to validate the 4π electron-counting and the concept of 5c–4e σ-bond.

4.3. Charge-state dependence of ring-like *versus* chain-like structures in $B_3N_2H_5^{0/-/2-}$

Ring-like C_{2v} $B_3N_2H_5^{0/-}$ (**1** and **2**) have proved to be global minima (Fig. 1), whereas C_{2v} $B_3N_2H_5^{2-}$ (**3**) is only a local minimum, being ∼21 kcal mol^{-1} above a chain-like C_s ($^1A'$) open structure. A relevant chain-like isomer can be traced back in $B_3N_2H_5^{0/-}$ as well. The energetics of these two sets of structures are compared in Fig. 5 at three charge-states; note that the open structure of $B_3N_2H_5$ differs slightly from those of $B_3N_2H_5^{-/2-}$ in the position of one H atom. From neutral species to monoanion, the ring-like isomer remains as global minimum. However, at the dianion charge-state, the chain-like isomer gains relative stability and becomes the global minimum, and indeed the top six isomers of $B_3N_2H_5^{2-}$ are all chain-like (Fig. S3, ESI†). Since the frontier CMOs of **2** and **3** are the same, the reverse energy order from monoanion and dianion has to be attributed to the enhanced intramolecular Coulomb repulsion in dianion **3**.

Calculated natural charges for **1–3** (Table 3) indicate that 84% of the first extra charge, and 97% of the second, are distributed on B1/B3/B2. In particular, the B1/B3 centers accept 65% and 48% of the first and second charges, respectively, which should impose substantial Coulomb repulsion in **3**. Understandably, chain-like $B_3N_2H_5^{2-}$ can better manage the charges. Coulomb repulsion has already a discernible structural effect in monoanion **2** (Fig. 1), for which the B1–N8/B3–N7 bonds are elongated. For dianion **3**, the B1–B3 bond does not shrink despite the gain of electron in the vicinity, further manifesting the repulsive effect in the ring.

Fig. S4 (ESI†) illustrates the chain-like C_s ($^1A'$) structure of $B_3N_2H_5^{2-}$ at the B3LYP level. The B–N distances (from left to right) of 1.36/1.38, 1.27, and 1.50 Å are assigned to double B=N, triple B≡N, and single B–N bonds, respectively,[37] which lead to a classical Lewis structure as shown in Fig. S4(b) (ESI†). The Lewis presentation is fully confirmed by the AdNDP data (Fig. S5, ESI†). The two extra charges are located primarily on two N centers (26% *versus* 43%).

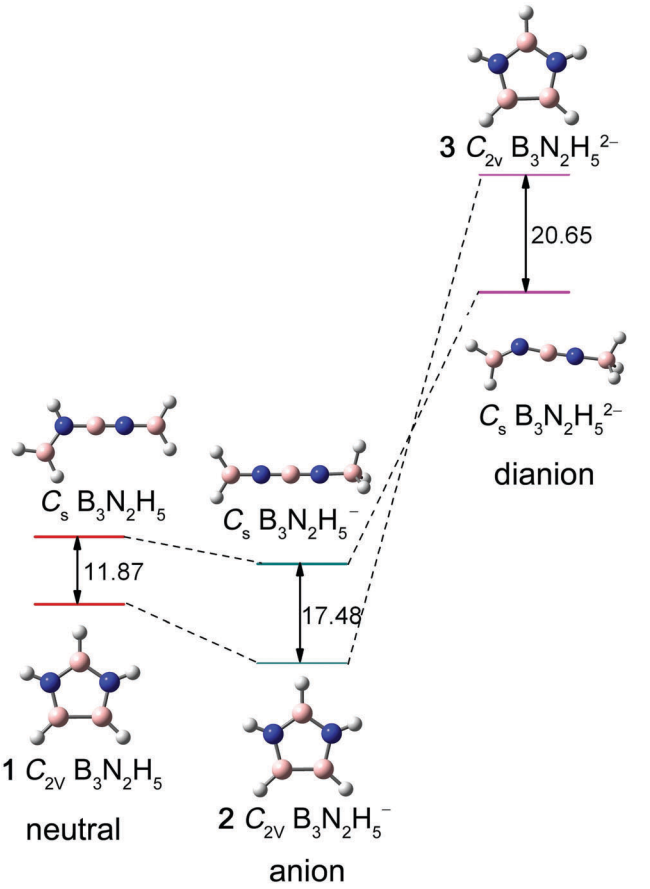

Fig. 5 Diagram for the energetics of two isomeric structures, ring-like (**1**–**3**) *versus* chain-like, in three charge-states. Relative energies (in kcal mol^{-1}) are shown at the B3LYP/aug-cc-pVTZ level.

Table 3 Calculated natural charges (in |e|) for C_{2v} $B_3N_2H_5$ (**1**), $B_3N_2H_5^-$ (**2**), and $B_3N_2H_5^{2-}$ (**3**) at the B3LYP/aug-cc-pVTZ level

Species	B1(B3)[a]	B2[a]	H4	H5(H6)	N7(N8)	H9(H10)
C_{2v} $B_3N_2H_5$ (**1**)	**+0.406**	**+0.807**	−0.083	−0.084	−1.080	+0.360
C_{2v} $B_3N_2H_5^-$ (**2**)	**+0.080**	**+0.613**	−0.126	−0.115	−1.069	+0.360
C_{2v} $B_3N_2H_5^{2-}$ (**3**)	**−0.159**	**+0.121**	−0.128	−0.121	−1.064	+0.346

[a] Centers with substantial changes of natural charges from neutral to anion and dianion are shown in boldface.

4.4. Predicted infrared spectrum and photoelectron spectrum

To aid future experimental characterizations of the C_{2v} $B_3N_2H_5$ (**1**, $^1A_1$) and $B_3N_2H_5^-$ (**2**, $^2B_1$) global-minimum clusters, we report their calculated infrared (IR) spectrum and photoelectron spectrum, respectively. The IR simulation of **1** is presented in Fig. 6. Three adjacent peaks are revealed at 2611–2647 cm^{-1}, which correspond to B–H symmetric stretchings. Among them, the intense peak at 2627 cm^{-1} (a_1) is associated with terminal B1–H and B3–H stretching. Another four adjacent peaks are present at 1273–1394 cm^{-1}, mainly corresponding to B–H rocking vibrations. We also calculated the vertical ionization potential (VIP) of **1**, which amounts to 10.06 eV at the B3LYP level (Table 4).

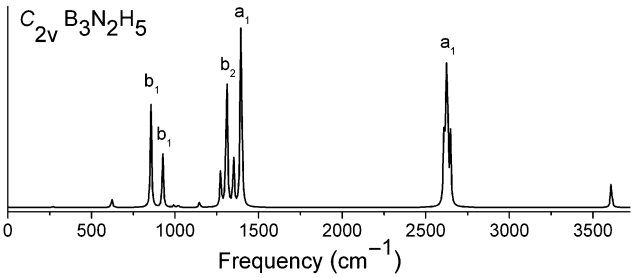

Fig. 6 Simulated infrared (IR) spectrum of C_{2v} $B_3N_2H_5$ (**1**) neutral species.

Table 4 Calculated lowest vibrational frequencies (ν_{min}), vertical ionization potentials (VIPs), and formation energies (FEs) of C_{2v} $B_3N_2H_5$ (**1**), C_{2v} $B_3N_2H_5^-$ (**2**), and their relevant sandwich-type complexes (**6–9**). For comparison, those of the cyclopentadienyl counterparts, D_{5d} $(C_5H_5)_2Fe$ (**4**) and D_{5h} $(C_5H_5)_2Fe$ (**5**), have also been tabulated

Complexes	ν_{min} (cm^{-1})	VIP (eV)	FE[a] (kcal mol^{-1})
C_{2v} $B_3N_2H_5$ (**1**)	270.22	10.06	
C_{2v} $B_3N_2H_5^-$ (**2**)	374.74	0.51	
D_{5d} $(C_5H_5)_2Fe$ (**4**)	−40.37	7.05	−192.17
D_{5h} $(C_5H_5)_2Fe$ (**5**)	31.97	7.06	−192.56
C_{2h} $[(B_3N_2H_5)_2Fe]^{2-}$ (**6**)	57.68		3.60[b]
C_{2v} $[(B_3N_2H_5)_2Fe]^{2-}$ (**7**)	−54.35		
C_{2h} $[(B_3N_2H_5)_2Fe]Li_2$ (**8**)	51.78	5.77	−113.24[b]
C_{2v} $[(B_3N_2H_5)_2Fe]Li_2$ (**9**)	−10.77		

[a] Free energy corrections are included in the FE calculations. [b] The difference in FE between **6** and **8**, as well as between **7** and **9**, is attributed to intramolecular Coulomb repulsion in **6** and **7** due to the multiple charges.

Anion photoelectron spectroscopy (PES) probes the electron affinity of a neutral species, accessing the neutral ground state and low-lying excited states. The calculated ground-state adiabatic and vertical detachment energies (ADE and VDE) of $B_3N_2H_5^-$ (**2**) are 0.37 and 0.51 eV, respectively, at B3LYP, which are refined to 0.25 and 0.38 eV at single-point CCSD(T). These values turn out to be much smaller than those of the isovalent $B_3S_2H_3^-$ cluster (ADE: 1.81 eV, VDE: 1.98 eV; single-point CCSD(T) data),[18b] indicating that $B_3N_2H_5^-$ (**2**) should be less stable than $B_3S_2H_3^-$. The simulated PES spectrum of **2**, based on B3LYP and TD-B3LYP calculations, is shown in Fig. 7. Nine detachment channels are found with VDEs from 0.51 to 6.28 eV. This PES spectrum features an extremely low first VDE and a sizable energy gap (~3.3 eV), both indicating that the corresponding neutral species, $B_3N_2H_5$ (**1**), is electronically robust, which reinforces the concept of the 5c–4e o-bond (see Section 4.2.).

4.5. C_{2v} $B_3N_2H_5^-$ (2) as a potential ligand in sandwich-type complexes

Ferrocene, D_{5h} $(C_5H_5)_2Fe$, in which cyclopentadienyl C_5H_5 serves as ligand, was first prepared in the early 1950s.[17,41–44] C_{2v} $B_3N_2H_5^-$ (**2**) is isovalent to cyclopentadienyl. We thus attempt to pursue sandwich-type complexes by using **2** as ligand. Fig. 8 depicts the optimized structures of C_{2h} $[(B_3N_2H_5)_2Fe]^{2-}$ (**6**), C_{2v} $[(B_3N_2H_5)_2Fe]^{2-}$ (**7**), C_{2h} $[(B_3N_2H_5)_2Fe]Li_2$ (**8**), and C_{2v} $[(B_3N_2H_5)_2Fe]Li_2$ (**9**) complexes at the B3LYP level, as compared

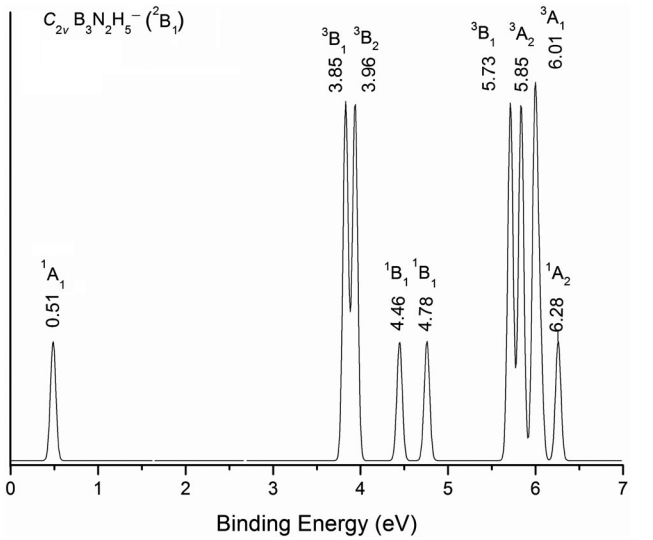

Fig. 7 Simulated photoelectron spectrum of C_{2v} $B_3N_2H_5^-$ (**2**) cluster at the time-dependent B3LYP (TD-B3LYP) level with the aug-cc-pVTZ basis set. The simulation was done by fitting the distribution of calculated vertical detachment energies (VDEs) with unit-area Gaussian functions of 0.04 eV half-width.

with the cyclopentadienyl counterparts: D_{5d} $(C_5H_5)_2Fe$ (**4**) and D_{5h} $(C_5H_5)_2Fe$ (**5**). Structural integrity of **2** is preserved in complexes **6–9**. Differing from staggered **4** and eclipsed **5**, the staggered **6** is a true minimum with the lowest vibrational frequency of 57.68 cm^{-1} and it is more stable with respect to eclipsed **7** (Table 4). Complex **6** follows the 18-electron rule.

When two Li^+ cations are attached to dianions **6** and **7**, neutral salt complexes C_{2h} $[(B_3N_2H_5)_2Fe]Li_2$ (**8**) and C_{2v} $[(B_3N_2H_5)_2Fe]Li_2$ (**9**) with a planar $B_3N_2H_5^-$ motif are obtained. Complex **8** is a true minimum with the lowest frequency of 51.78 cm^{-1}. Both **7** and **9** are transition states. The calculated VIP of **8** is 5.77 eV at B3LYP, a value that is slightly lower than that of **5** (7.06 eV).

To further evaluate the thermodynamic stability of sandwich complexes **6** and **8**, we have calculated their formation energies (FEs) following the equations:

$$Fe\ (^5A_{1g}) + 2B_3N_2H_5^-(\mathbf{2},\ C_{2v},\ ^2B_1) = [(B_3N_2H_5)_2Fe]^{2-}(\mathbf{6},\ C_{2h},\ ^1A_g)$$

$$2Li^+\ (^1A_{1g}) + [(B_3N_2H_5)_2Fe]^{2-}\ (\mathbf{6},\ C_{2h},\ ^1A_g) = [(B_3N_2H_5)_2Fe]Li_2\ (\mathbf{8},\ C_{2h},\ ^1A_g)$$

In the calculations of FEs, free energy corrections are considered. As shown in Table 4, the FEs are 3.60 and −113.24 kcal mol^{-1} for **6** and **8**, respectively. The FE for **8** is substantial, indicating that its formation is highly exothermic. Note that the FEs of D_{5h} $(C_5H_5)_2Fe$ (**5**) and C_{2h} $[(B_3S_2H_3)_2Fe]Li_2$ (ref. 18*b*) at the same level are −192.56 and −87.60 kcal mol^{-1}, respectively. Thus, $B_3N_2H_5^-$ (**2**) is probably a more favorable ligand than $B_3S_2H_3^-$. Similar to D_{5h} $(C_5H_5)_2Fe$,[17] η^4-heterocyclic $(C_2P_2R_2)_2Ni$ sandwiches,[45,46] and metal–benzene complexes $M_n(benzene)_m$ (M = Sc to Cu),[47] sandwiches **6** and **8** (especially **8**) may be viable targets for synthetic efforts.

We have also attempted to use C_{2v} $B_3N_2H_5$ (**1**) as a ligand to build sandwich complexes, for which the same metal Fe,

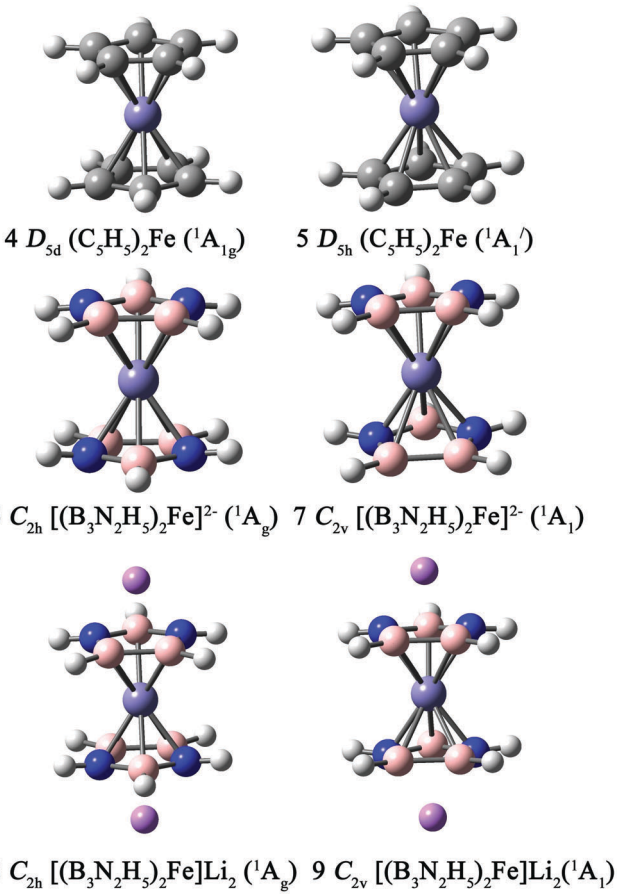

Fig. 8 Sandwich-type complexes C_{2h} $[(B_3N_2H_5)_2Fe]^{2-}$ (**6**), C_{2v} $[(B_3N_2H_5)_2Fe]^{2-}$ (**7**), C_{2h} $[(B_3N_2H_5)_2Fe]Li_2$ (**8**), and C_{2v} $[(B_3N_2H_5)_2Fe]Li_2$ (**9**) at the B3LYP level, as compared with their cyclopentadienyl counterparts (**4** and **5**). The B atom is in pink, N in blue, and C and H in gray.

basis set, and method are chosen. Sandwich-type C_{2h} $[(B_3N_2H_5)_2Fe]$ complex (with 16 electrons) turns out to be a second order saddle point, with imaginary frequencies of −158.71 and −36.70 cm^{-1}. The failure may be attributed to the fact that $[(B_3N_2H_5)_2Fe]$ does not satisfy the 18-electron rule. The corresponding C_{2v} $[(B_3N_2H_5)_2Fe]$ complex is a true minimum, yet there exists apparent structural distortion so that the two $B_3N_2H_5$ ligands are not parallel to each other. The N8B2N7 edges of the ligands are brought closer with respect to the B1B2 edges, akin to a seashell with mouth slightly opening.

It is possible to tune the electron counting of sandwich complexes *via* the metal center. For example, the Ni center has two more electrons than Fe and thus the $[(B_3N_2H_5)_2Ni]$ neutral complex is an 18-electron system. Fig. S6 (ESI†) depicts the optimized structures of C_{2h} $[(B_3N_2H_5)_2Ni]$ (^1A_g) and C_{2v} $[(B_3N_2H_5)_2Ni]$ ($^1A_1$) at the B3LYP level. The staggered C_{2h} sandwich is a true minimum with the lowest vibrational frequency of 114.27 cm^{-1}, which is more stable (by 6.07 kcal mol^{-1}) than the eclipsed C_{2v} complex. The latter is also a minimum. It shows again certain distortion with the two ligands being nonparallel to each other. We comment here that the structural distortions in C_{2v} $[(B_3N_2H_5)_2Fe]$ and C_{2v} $[(B_3N_2H_5)_2Ni]$ demonstrate intriguing intramolecular electrostatic interactions even in the neutral sandwich complexes.

5. Conclusions

We have reported theoretical predictions, at the B3LYP and single-point CCSD(T) levels, of boron-nitrogen hydride clusters C_{2v} $B_3N_2H_5^{0/-}$ (**1** and **2**) as global minima *via* structural searches, as well as C_{2v} $B_3N_2H_5^{2-}$ (**3**) as a local minimum, and studied their electronic structure and chemical bonding. C_{2v} $B_3N_2H_5$ (**1**) with a pentagonal B_3N_2 core is a 4π system in a bonding/nonbonding combination, akin to that of a prototypical three-center four-electron ω-bond. We propose the concept of a five-center four-electron o-bond, where the 4π electron-counting in **1** is robust. In contrast, 6π is not favorable for the $B_3N_2H_5^{0/-/2-}$ system. The concept may be applicable for other heteroatomic, pentagonal clusters and molecules.

Acknowledgements

This work was supported by the National Natural Science Foundation of China (21573138), the Natural Science Foundation of Shandong Province (ZR2014BL011), the Research Fund of Binzhou University (2014ZDL03), and the State Key Laboratory of Quantum Optics and Quantum Optics Devices (KF201402).

References

1 L. Barton, F. A. Grimm and R. F. Porter, *Inorg. Chem.*, 1966, **5**, 2076.
2 W. Harshbarger, G. Lee, R. F. Porter and S. H. Bauer, *Inorg. Chem.*, 1969, **8**, 1683.
3 P. W. Fowler and E. Steiner, *J. Phys. Chem. A*, 1997, **101**, 1409.
4 J. J. Engelberts, R. W. A. Havenith, J. H. van Lenthe, L. W. Jenneskens and P. W. Fowler, *Inorg. Chem.*, 2005, **44**, 5266.
5 C. H. Chang, R. F. Porter and S. H. Bauer, *Inorg. Chem.*, 1969, **8**, 1689.
6 J. A. Tossell and P. Lazzeretti, *J. Phys. Chem.*, 1990, **94**, 1723.
7 K. L. Bhat, G. D. Markham, J. D. Larkin and C. W. Bock, *J. Phys. Chem. A*, 2011, **115**, 7785.
8 S. H. Bauer, *J. Am. Chem. Soc.*, 1938, **60**, 524.
9 D. Z. Li, H. Bai, Q. Chen, H. G. Lu, H. J. Zhai and S. D. Li, *J. Chem. Phys.*, 2013, **138**, 244304.
10 (*a*) H. J. Zhai, Q. Chen, H. Bai, S. D. Li and L. S. Wang, *Acc. Chem. Res.*, 2014, **47**, 2435; (*b*) H. J. Zhai, S. D. Li and L. S. Wang, *J. Am. Chem. Soc.*, 2007, **129**, 9254; (*c*) S. D. Li, H. J. Zhai and L. S. Wang, *J. Am. Chem. Soc.*, 2008, **130**, 2573.
11 (*a*) D. Z. Li, S. G. Zhang, J. J. Liu and C. Tang, *Eur. J. Inorg. Chem.*, 2014, 3406; (*b*) D. Z. Li, C. C. Dong and S. G. Zhang, *J. Mol. Model.*, 2013, **19**, 3219.
12 (*a*) N. C. Baird and R. K. Datta, *Inorg. Chem.*, 1972, **11**, 17; (*b*) N. C. Baird, *Inorg. Chem.*, 1973, **12**, 473.
13 A. J. Bridgeman and J. Rothery, *Inorg. Chim. Acta*, 1999, **288**, 17.
14 D. Z. Li, L. J. Zhang, T. Ou, H. X. Zhang, L. Pei, H. J. Zhai and S. D. Li, *Phys. Chem. Chem. Phys.*, 2015, **17**, 16798.

15 W. J. Tian, X. R. You, D. Z. Li, T. Ou, Q. Chen, H. J. Zhai and S. D. Li, *J. Chem. Phys.*, 2015, **143**, 064303.
16 D. Z. Li, S. G. Zhang and C. C. Dong, *Eur. J. Inorg. Chem.*, 2016, 1103.
17 T. J. Kealy and P. L. Pauson, *Nature*, 1951, **168**, 1039.
18 (*a*) D. Z. Li, H. Bai, T. Ou, Q. Chen, H. J. Zhai and S. D. Li, *J. Chem. Phys.*, 2015, **142**, 014302; (*b*) D. Z. Li, R. Li, L. J. Zhang, T. Ou and H. J. Zhai, *Phys. Chem. Chem. Phys.*, 2016, **18**, 21412.
19 F. Weinhold and C. R. Landis, *Valency and Bonding: A Natural Bond Orbital Donor–Acceptor Perspective*, Cambridge University Press, Cambridge, 2005, pp. 275–306.
20 A. P. Sergeeva, B. B. Averkiev, H. J. Zhai, A. I. Boldyrev and L. S. Wang, *J. Chem. Phys.*, 2011, **134**, 224304.
21 (*a*) M. Saunders, *J. Comput. Chem.*, 2004, **25**, 621; (*b*) P. P. Bera, K. W. Sattelmeyer, M. Saunders, H. F. Schaefer III and P. v. R. Schleyer, *J. Phys. Chem. A*, 2006, **110**, 4287.
22 A. N. Alexandrova, A. I. Boldyrev, Y. J. Fu, X. Yang, X. B. Wang and L. S. Wang, *J. Chem. Phys.*, 2004, **121**, 5709.
23 A. N. Alexandrova and A. I. Boldyrev, *J. Chem. Theory Comput.*, 2005, **1**, 566.
24 A. D. Becke, *J. Chem. Phys.*, 1993, **98**, 5648.
25 C. Lee, W. T. Yang and R. G. Parr, *Phys. Rev. B: Condens. Matter Mater. Phys.*, 1988, **37**, 785.
26 J. Cizek, *Adv. Chem. Phys.*, 1969, **14**, 35.
27 (*a*) G. E. Scuseria and H. F. Schaefer III, *J. Chem. Phys.*, 1989, **90**, 3700; (*b*) G. E. Scuseria, C. L. Janssen and H. F. Schaefer III, *J. Chem. Phys.*, 1988, **89**, 7382.
28 J. A. Pople, M. Head-Gordon and K. Raghavachari, *J. Chem. Phys.*, 1987, **87**, 5968.
29 Stuttgart RSC 1997 ECP basis sets used in this work and the related references therein can be obtained from https://bse.pnl.gov/bse/portal.
30 D. Y. Zubarev and A. I. Boldyrev, *Phys. Chem. Chem. Phys.*, 2008, **10**, 5207.
31 P. v. R. Schleyer, C. Maerker, A. Dransfeld, H. J. Jiao and N. J. R. v. E. Hommes, *J. Am. Chem. Soc.*, 1996, **118**, 6317.
32 E. D. Glendening, J. K. Badenhoop, A. E. Reed, J. E. Carpenter, J. A. Bohmann, C. M. Morales and F. Weinhold, *NBO 5.0*, Theoretical Chemistry Institute, University of Wisconsin, Madison, WI, 2001.
33 M. E. Casida, C. Jamorski, K. C. Casida and D. R. Salahub, *J. Chem. Phys.*, 1998, **108**, 4439.
34 R. Bauernschmitt and R. Ahlrichs, *Chem. Phys. Lett.*, 1996, **256**, 454.
35 M. J. Frisch, G. W. Trucks, H. B. Schlegel, G. E. Scuseria, M. A. Robb, J. R. Cheeseman, G. Scalmani, V. Barone, B. Mennucci, G. A. Petersson, H. Nakatsuji, M. Caricato, X. Li, H. P. Hratchian, A. F. Izmaylov, J. Bloino, G. Zheng, J. L. Sonnenberg, M. Hada, M. Ehara, K. Toyota, R. Fukuda, J. Hasegawa, M. Ishida, T. Nakajima, Y. Honda, O. Kitao, H. Nakai, T. Vreven, J. A. Montgomery, Jr., J. E. Peralta, F. Ogliaro, M. Bearpark, J. J. Heyd, E. Brothers, K. N. Kudin, V. N. Staroverov, R. Kobayashi, J. Normand, K. Raghavachari, A. Rendell, J. C. Burant, S. S. Iyengar, J. Tomasi, M. Cossi, N. Rega, J. M. Millam, M. Klene, J. E. Knox, J. B. Cross, V. Bakken, C. Adamo, J. Jaramillo, R. Gomperts, R. E. Stratmann, O. Yazyev, A. J. Austin, R. Cammi, C. Pomelli, J. W. Ochterski, R. L. Martin, K. Morokuma, V. G. Zakrzewski, G. A. Voth, P. Salvador, J. J. Dannenberg, S. Dapprich, A. D. Daniels, Ö. Farkas, J. B. Foresman, J. V. Ortiz, J. Cioslowski and D. J. Fox, *GAUSSIAN 09, Revision D.01*, Gaussian, Inc., Wallingford, CT, 2009.
36 T. Lu and F. W. Chen, *Acta Chim. Sin.*, 2011, **69**, 2393.
37 P. Pyykkö, *J. Phys. Chem. A*, 2015, **119**, 2326.
38 Q. Chen, H. G. Lu, H. J. Zhai and S. D. Li, *Phys. Chem. Chem. Phys.*, 2014, **16**, 7274.
39 A. Rehaman, A. Datta, S. S. Mallajosyula and S. K. Pati, *J. Chem. Theory Comput.*, 2006, **2**, 30.
40 K. J. Iversen, D. J. D. Wilson and J. L. Dutton, *Chem. – Eur. J.*, 2014, **20**, 14132.
41 R. Zhang, Y. J. Ji, L. Yang, Y. Zhang and G. C. Kuang, *Phys. Chem. Chem. Phys.*, 2016, **18**, 9914.
42 Z. U. Abdin, L. Wang, H. J. Yu, M. Saleem, M. Akram, N. M. Abbasi, H. Khalid, R. L. Sun and Y. S. Chen, *New J. Chem.*, 2016, **40**, 3155.
43 L. Peng, A. C. Feng, M. Huo and J. Y. Yuan, *Chem. Commun.*, 2014, **50**, 13005.
44 Š. Toma, J. Csizmadiová, M. Mečiarová and R. Šebesta, *Dalton Trans.*, 2014, **43**, 16557.
45 M. D. Su and S. Y. Chu, *J. Phys. Chem.*, 1991, **95**, 9757.
46 T. Wettling, G. Wolmershäuser, P. Binger and M. Regitz, *J. Chem. Soc., Chem. Commun.*, 1990, **21**, 1541.
47 (*a*) T. Kurikawa, H. Takeda, M. Hirano, K. Judai, T. Arita, S. Nagao, A. Nakajima and K. Kaya, *Organometallics*, 1999, **18**, 1430; (*b*) A. Nakajima and K. Kaya, *J. Phys. Chem. A*, 2000, **104**, 176.

